ORIGINAL ARTICLE

Parametric study of solar power tower driven combined supercritical CO_2 cycle and organic Rankine cycle using low GWP fluids

R.S. Mishra, Yunis Khan

Department of Mechanical Engineering, Delhi Technological University, New Delhi, India

Abstract

In this study, parametric analysis of the solar power tower (SPT) driven combined recuperated supercritical CO_2 Brayton cycle and organic Rankine cycle (ORC) were carried out. Further, low global warming potential and zero ozone depletion fluids were considered in bottoming ORC to reduce harmful effects on environment. A computer program was made in engineering equation solver for simulation. The effects of the SPT design parameters such direct normal irradiation (DNI), concentration ratio (CR), receiver emittance and heat transfer fluid velocity on the system performance were investigated. It was found that thermal performance increased with DNI, CR and heat transfer fluid velocity while decreased with receiver emittance. At 0.95 kW/m^2 of DNI, R1224yd(Z) achieved the highest exergy efficiency, thermal efficiency and net power output of 58.52% and 54.43% and 293.50 kW, respectively. ©2021 ijrei.com. All rights reserved

1. Introduction

Electricity is still primarily produced in the modern world by burning traditional fuels like natural gas, oil, coal, and that not only has a finite lifespan but also emit liquid or gaseous contaminants during service. Solar energy has gained considerable attention as one of the most important candidates for replacing fossil fuels for electricity supply because it is an inexhaustible, renewable, and secure energy source [1, 2]. The initial technology and business planning for CSP (concentrating solar power) technologies such as the dish/engine, power tower, and parabolic trough have recently advanced rapidly around the world. Even then, CSP system's power production efficiencies have been observed as low, which consequently raises the capital expenditure of power production, and further technological innovation of CSP

systems must be prioritized. Solar Power Tower (SPT) is the most advanced technology in the CSP. SPT system comprises of a range of sophisticated sub-systems such as a recipient, a tower 75-150 m high and thermal (optional), a heliostat field of 50-150 m^2 and a power conversion system, per heliostat area. Solar radiation focuses on the heliostat receptor field where elevated temperatures heat is produced through a high energy cycle for power production and industrial process supply [3].

1.1 SPT driven cycles

Several SPT driven cycles studies have been performed including combined SCO_2 and trans critical CO_2 cycles [4]; SCO_2 and ORC pre-compression cycles [5]; CO_2 Brayton

cycles [6]; SCO_2 recompression with and without main compressor intercooling [7]; three-generation combined cycle [8]; and multi-generation combination cycles [9]. Cycles have been studied for several years. The SCO_2 cycle is a heat-use cycle that may use heat, including geothermal, solar thermal, coal-fueled and natural gas sources from a variety of sources [10]. Various studies were done on solar integrated SCO_2 cycles, such as Singh and Mishra's [11] study on the combined simple recuperated SCO_2 and ORC using parabolic trough solar collectors (PTSC). They discovered that the combined cycle's highest thermal efficiency and exergetic efficiency were found 43.49% and 78.07% at 0.95 kW/m^2 of heat flux, respectively with R407C. In another study, Singh and Mishra [12] investigated improved power generation using PTSC-driven combined recompression of SCO_2 cycle and ORC. At 0.5 kW/m^2 of solar irradiation, the R123-based recompression SCO_2-ORC gave highest exergy efficiency and thermal efficiency of 73.4% and 40.89%, respectively. Singh and Mishra [13] investigated a PTSC-driven simple recuperated SCO_2-VAR cogeneration system for simultaneously cooling and power production. They found that at a DNI of 0.96 kW/m^2, the highest thermal and exergy efficiency of PTSC were found about 33.9 percent and 65.32%, respectively. On the other hand, exergy destruction rate shows the reverse trend to exergy efficiency, and PTSC have the highest exergy destructions (i.e. 3696 kW). The PTSC operated partial heating SCO_2 ($PSCO_2$) cycle combined with ORC was parametrically analyzed by Khan and Mishra [14]. $PSCO_2$ system was found to be 1-3 percent more thermally efficient than the without partial heating cycle. Also, authors found that incorporating ORC into an existing $PSCO_2$ cycle thermal efficiency increased by 4.47 percent over the standalone $PSCO_2$ cycle. At 950 W/m^2 of solar irradiation, the combined cycle with R1233zd(E) had the highest exergy and thermal efficiency, with 83.26 and 48.61 percent, respectively. Apart from PTSC-driven sCO_2 cycles, a few studies focused on SPT-driven combined SCO_2 cycles have also been carried out, such as The SPT driven combination SCO_2 pre-compression cycle and ORC for waste heat recovery are the results of Khan and Mishra [5] investigation. They found that the use of ORC increases thermal efficiency and net power output of 4.52 and 4.51 percent respectively in the pre-compression cycle. The combined cycle energy, exergy and hottest thermal efficiency of the combination and greatest values of 278.5 kW, 74.06% and 51.83% at 1000 W/m^2 solar radiation with R227ea radiation are enhanced through solar irradiation. The recovery rate of waste heat increases with the efficiency of the heat exchanger. Its greatest value was 0.5673, based on R227ea, at 0.95 efficiencies. Khatoon and Kim [4] examined an SPT-driven combined power block system that was incorporated with solar field a thermal energy storage system. The combined system includes SCO_2 recompression Brayton cycle system as a topping cycle and trans critical CO_2 power cycle to recover waste heat. Due to better heat transfer characteristics and temperature glide merit and of the trans critical CO_2 power cycle were chosen over traditional waste heat recovery systems to use other working fluids. Khan and Mishra [1] used ultra-

low GWP fluids to conduct a thermo-economic study of the pre-compression SCO_2 cycle with the ORC as bottoming driven by SPT system. Based on the findings, they concluded that HFO performed better than R134a. At 950 W/m^2 of solar irradiation, R1336mzz(Z) had the highest exergy efficiency, thermal efficiency and power output for the combined cycle with 59.60%, 55.02%, and 298.5kW, respectively. The R1336mzz(Z) fluid had the highest waste heat recovery ratio of 0.84, while R134a had just 0.099 at 0.95 heat exchanger effectiveness. Finally, the R1336mzz(Z) and R1234ze(Z) estimated the lowest and highest specific investment costs (SIC), respectively, 2234 and 2290 €/kWe.

Because of its low to medium temperature range, ORC is the best technology for recovering waste heat. Recent research has been done in this area, such as Yagli et al. [15], who used the benefits of the ORC to enhance the net output of a simple gas turbine (GT) situated in a wood production industry. A steam boiler is also connected to the GT in addition to the ORC to boost overall efficiency and generate required steam. Working fluids used in the analysis included toluene, R601, R123, R600, R11 benzene, hexane and cyclohexane. Highest thermal and exergy efficiency of the of the cogeneration system were found 69.19% and 75.51% at ORC turbine inlet parameters. Song et al. [16] proposed a hybrid system for recovering the waste heat from the internal combustion engine (ICE) that integrates the SCO_2 cycle system using the ORC as bottoming cycle from recovering residual heat from the system and from jacket water and exhaust gas. Finally, they estimated that, based on a reference case involving a standalone SCO_2 system for an ICE with 1170 kW of a rated power output, the combined cycle system can produce a maximum net power output of 215 kW at a minimum SIC of 4670 $/kW, which is 58 and 4% more than a standalone SCO_2 power cycles, respectively. It has been found from the literature survey various study were performed on the combined simple SCO_2 Brayton cycle and ORC. However, no study was performed based on solar power tower driven simple recuperated SCO_2 Brayton cycle and ORC using low global warming potential (GWP) and zero ozone depletion potential (ODP) fluids to mitigate worst environmental effects. Therefore, present study deals with the parametric evaluation of the combined cycle. The effects of the SPT design parameters such as direct normal irradiation (DNI), concentration ratio, velocity of heat transfer fluid and receiver emittance on system performance were investigated.

1.2 System description

Current system consists three subsystems first STP system, second simple SCO_2 Brayton cycle and third ORC as bottoming cycle for recovering waste heat. SPT system drives the SCO_2 cycle, through the heat exchanger-1 (HEX1) it supplies heat to the SCO_2 Brayton cycle where power is produced by turbine. After the recuperate still some amount of heat is remaining, through heat exchanger-2 (HEX2) this waste heat recovered by the ORC, where, also some amount of power

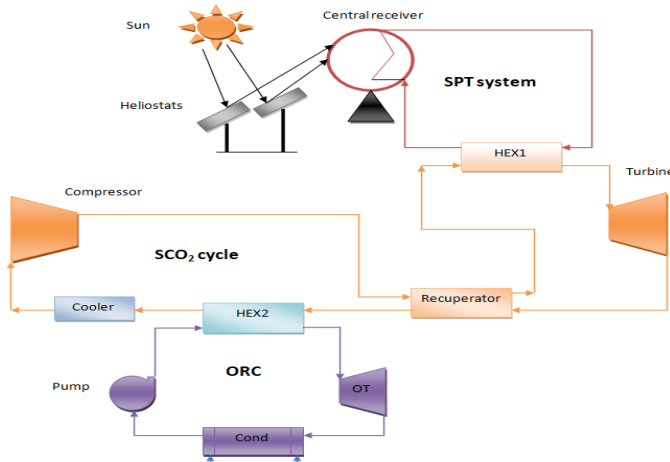is produced by the organic turbine (OT). The whole configuration has been shown in fig. 1.

Figure 1. Schematic diagram of SPT driven combined recuperated supercritical CO₂ cycle and ORC

2. Thermodynamic analysis

2.1 Assumptions

SPT powered combined cycle thermodynamic study has been conducted taking account of the following assumptions in support of simulation;

- All components of the system are in steady condition.
- In connecting pipes, friction, pressure and heat loss are overlooked
- Each component's potential and kinetic energy are insignificant
- Input data to facilitate simulation are shown in table 1 with the Heliostat and receiver settings constantly and assumed.
- Molten salt temperature inlet to the HEX1 has been taken 700°C [17].
- The maximum cycle temperature due to the thermal losses is 50 °C lower than the HEX-inlet salt temperature.
- In the recipients of a mass fraction of 32 percent and 68 percent molded salt HTF was employed in magnesium (MgC_{12}) and potassium chloride (KCl) mixture [4]. This HTF is the cheapest alternative compared to solar salt and liquid sodium [18] for the heliostat-driven SCO_2-cycle.
- It was also assumed that heliostat receives only beam irradiation.

2.2 Mathematical modeling

This part has established a thermal modelling equation of the proposed system based on the preservation of exergy and energy equations, taking the assumptions stated in the prior section into consideration. Modeling equations for SPT have been taken from the previous studies [1,2,4]. The control volume of each component has also been considered.

Heliostat fields are defined as direct sun heat incidences;

$$\dot{Q}_{solar} = DNI \cdot A_h \cdot N_h \qquad (1)$$

Table 1: Input parameters of the proposed model

SPT operational and geometric parameters [1]	
Direct normal irradiation	850 W/m² [11]
Temperature of Sun	5800K [19]
Solar multiple	2.8 [4]
Heliostat efficiency	58.71 % [20]
Number of heliostat	141 [21]
Initial temperature difference	15 K [4]
Heliostat's total mirror area	9.04×7.89 [4]
Convective heat loss coefficient	10 W/m²-K [20]
Solar receiver's temperature approach	423.15 K [20]
Concentration ratio	900 [20]
Convective heat loss factor	1 [20]
Tower height	74.62 m [21]
Absorptance	0.95 [21]
View factor	0.8 [21]
Thermal emittance	0.85 [21]
Combined cycle input data	
SCO₂ turbine inlet pressure	25 MPa [22]
SCO₂ inlet temperature	650 °C [4,22]
Compressor inlet temperature	32 °C [22, 17]
Compressor inlet pressure	7.5 MPa [22,17]
Compressor isentropic efficiency	0.85 [22,17]
SCO₂ turbine isentropic efficiency	0.88 [22, 17]
SCO₂ topping cycle mass flow rate	1.6 kg/s
Heat exchanger/recuperator effectiveness	0.95 [1,2]
ORC turbine inlet pressure	3 MPa [1,2,11]
Mass flow rate in bottoming ORC	2.7 kg/s
ORC pump's Isentropic efficiency	0.7 [23]
ORC turbine's Isentropic efficiency	0.8 [23]

Where direct normal irradiation (DNI) is DNI, A_h shall be the single area of heliostat (m²), and N_h shall be the number of the heliostats. However, part of this heat is lost in the environment due to the efficiency of the heliostat. The exact amount of heat generated by the field of heliostat is thus given as;

$$\dot{Q}_h = \dot{Q}_{solar} \cdot \eta_h \qquad (2)$$

Where η_h is heliostat's efficiency. The heat is sent in this quantity to the solar receiver where the fluid is transferred. But some of the heat is lost in the atmosphere. Therefore, the heat available at the recipient of the solar center is determined;

$$\dot{Q}_r = \dot{Q}_h \cdot \eta_r = \dot{Q}_h - \dot{Q}_{loss,r} \qquad (3)$$

Where, η_r is the receiver thermal efficiency, is defined as;

$$\eta_r = \alpha - \frac{\zeta \cdot f_{view} \cdot \sigma \cdot T_R{}^4 + h_{conv} \cdot f_{conv} \cdot (T_R - T_{air})}{DNI \cdot \eta_h \cdot CR} \qquad (4)$$

Where, T_R is the surface temperature of the receiver and CR

is known concentrated ratio. ζ is the solar emittance. For computing the heat loss, the following expression is used.

$$T_R = T_1 + \delta T_R \tag{5}$$

T_1 is the temperature of the turbine inlet and δT_R is the solar receptor approach temperature.

The solar receiver and the heliostat field are listed in table 1 with operational and geometric specifications.

Moreover, the exergy of any system can be explained as the utmost effort that the system can achieve when the system reaches its dead circumstances. The equation of exergy balance can be established as control volume [24];

$$\sum \left(1 - \frac{T_0}{T_J}\right)\dot{Q}_J - \dot{W}_{cv} - \sum(\dot{m}_i E_i) - \sum(\dot{m}_e E_e) - \dot{E}D = 0 \tag{6}$$

Where, $\dot{E}D$ is the rate of exergy degradation, and j relates in a particular State to thermal property. The combined system is determined by the solar exergy inflow by Petela's formula [25];

$$\dot{E}_{solar} = \dot{Q}_{solar} \cdot \left[1 + \frac{1}{3}\left(\frac{T_0}{T_{su}}\right)^4 - \frac{4}{3}\left(\frac{T_0}{T_{su}}\right)\right] \tag{7}$$

Where, T_{su} and T_0 are the sun and reference temperature respectively. The useful exergy found by the molten salt in the receiver, is calculated as

$$\dot{E}_r = \dot{m}_{ms} \cdot Cp_{ms} \cdot \left[(T_b - T_a) - \left(T_0 \cdot \ln\frac{T_b}{T_a}\right)\right] \tag{8}$$

Assuming throughout constant system chemical exergy and neglecting energy due to velocity and height, the specific physical exergy at j^{th} point is defined as [24];

$$E_j = (h_j - h_0) - T_0(h_j - s_0) \tag{9}$$

Net power output obtained from the combined cycle is defined as;

$$\dot{W}_{net} = \dot{W}_T + \dot{W}_{OT} - \dot{W}_{Comp} - \dot{W}_{pump} \tag{10}$$

Solar powered combined cycle's thermal efficiency is determined as;

$$\eta_{th} = \frac{\dot{W}_{net}}{\dot{Q}_{solar}} \tag{11}$$

The exergy analysis of the combined system using second law of thermodynamics is derived here. The exergy destruction in each component is determined by applying the exergy balance equation (6) for each component after assuming no heat loss in the component [24]. When the exergy destruction rate for each component has been computed, the combined cycle total exergy destruction rate is calculated as;

$$\dot{E}D_{Total} = \dot{E}D_{HEX1} + \dot{E}D_T + \dot{E}D_{OT} + \dot{E}D_{recup} + \dot{E}D_{comp} + \dot{E}D_{cooler} + \dot{E}D_{pump} + \dot{E}D_{HEX2} + \dot{E}D_{cond} + \dot{E}D_{reciever} \tag{12}$$

On the basis of the thermal modeling, numerous mathematical relations are used in the performance analysis of the solar power tower powered combined cycle have been discussed below;

Combined cycle exergy efficiency is determined as [1,2,11,24];

$$\eta_{ex} = 1 - \frac{\dot{E}D_{Total}}{\dot{E}_{solar}} \tag{13}$$

Or

$$\eta_{ex} = \frac{\dot{W}_{net}}{\dot{E}_{solar}} \tag{14}$$

The combined cycle's thermal efficiency can also be defined by the relation between thermal and exergy efficiency of the combined cycle [24];

$$\eta_{th} = \eta_{ex} \cdot \eta_{Carnot} \tag{15}$$

In the SPT powered combined cycle the thermal modeling equations were solved using engineering equation solver (EES) [26].

2.3 Working fluid selection

Working fluids for any device should really be carefully selected because they have an effect on the environment, economic feasibility, and long-term viability. In the receiver, molten salt HTF was made up of a mixture of magnesium dichloride (MgC_{l2}) and potassium chloride (KCl), with mass fractions of 32% and 68%, respectively [4]. This HTF was chosen because, when compared to solar salt and liquid sodium (Na), it is the most cost-effective option for the heliostat-driven sCO_2 cycle [27]. This molten salt's thermo-physical properties in reference Khan and Mishra (2020a). The ORC's working fluid is difficult to select because it loses chemical stability above its optimum temperature, but it achieves the best thermo-physical properties at the right pressure and temperature [18]. To choose suitable fluids for the analysis, various parameters, critical points, such as GWP, thermal stability, and ozone depletion potential (ODP), were analyzed. High GWP fluids, such as hydro fluoro carbons (HCFCs), and high ODP fluids, such as CFCs (chloro fluoro carbons) were replaced by HFO fluids which has ultra-low GWP and ultra-low ODP because GWP is limited at under 150, as restrictions like the European Union [28] prohibit it. Working fluids are called dry, isentropic and moist fluids for the ORC system. Because the expander outlet has high-quality vapour, dry and insulating work is more suited than other fluid. In the present investigation too, the waste heat supply has a low temperature.

This analysis was therefore carried out on the ORC analytics based on nine HFO working fluids such as R1234ze(Z), R1224yd(Z), R1225ye(Z), R1233zd(E), R1234yf, R1243zf, R1234ze(E) and R1336mzz(Z). Flame worthiness, with or without suffix. Normally two classes of toxicity such as lower toxicity (Class A) and higher toxicity (Class B) have been described. There are four flammability classes: 1, 2L, 2 or 3 [29]

2.4 Validation of the proposed cycle

In order to ensure the correct use of the modeling equation, previous studies were used to validate the current cycles. Thermal efficiency has been taken as the validation parameter for both the cycles. Present combined (SCO₂-ORC) cycle was validated with the previous study Singh and Mishra [11] at same baseline conditions respective to references. Thermal efficiency of the cycle was found nearly to the respective previous research as shown in table 2. However, present study was performed with input parameters that are different from the previous studies those were used for the validation purpose.
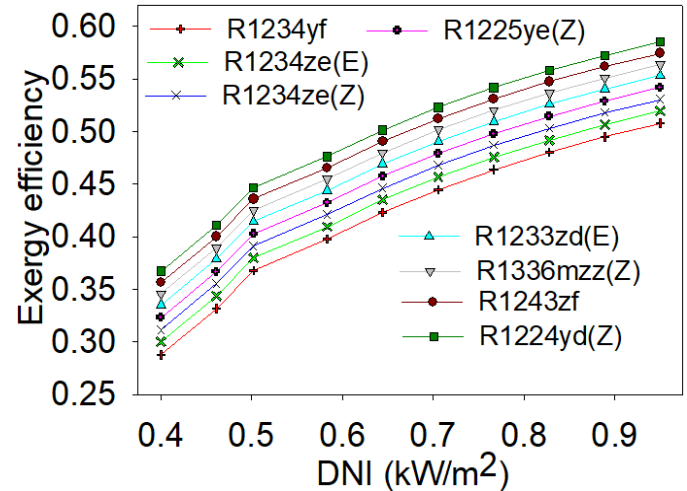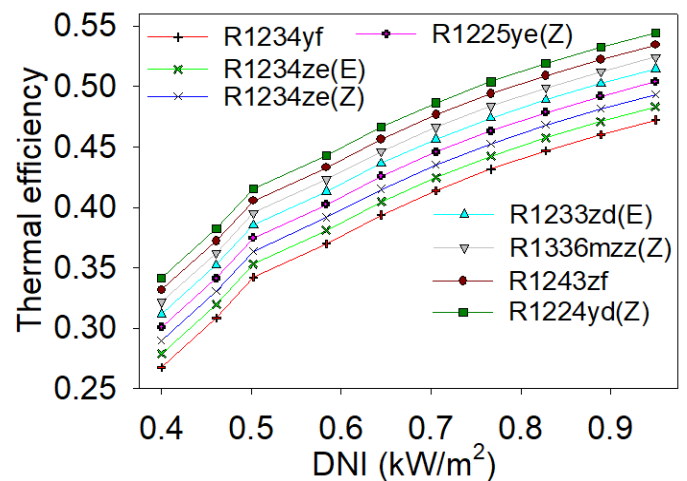
Table.2. Validation of combined (SCO₂-ORC) cycle

S. No	Baseline conditions.	Thermal efficiency Singh and Mishra [11]	Thermal efficiency Current model	Estimated error
1	Cycle maximum pressure = 25 MPa, Cycle maximum temperature = 400℃, Compressor inlet pressure = 7.4 MPa, Compressor inlet temperature =54.35 ℃, OT inlet pressure=3MPa η_{comp} =0.89, $\eta_{Turbine}$ =0.9 Working fluid in ORC=R245fa	52.03%	52.49%	0.76%

3. Results and discussions

Present study deals with parametric analysis of the SPT driven SCO₂ and ORC system using low GWP fluids. Results were calculated with computational technique considering assumptions and listed data in table 1.

3.1 Influence of the solar irradiation on the system performance

The basic condition for sun irradiation in the Indian climate in Mumbai was 850 W/m2. The impacts of solar irradiation on the efficiency of the system consequently need to be examined, since the current integrated model is powered by a solar power tower. The combined cycle's exergy efficiency was steadily raised with solar irradiation. This is explained by the efficient use of increased solar irradiation on the solar concentrate field. This correlates to an increase in the combined cycle inlet exergy [30].

With solar irradiation, power output and thermal efficiency of the system have also increased. At 950 W/m^2 of solar irradiation, R1224yd(Z) achieved the highest exergy efficiency, thermal efficiency and net power output of 58.52% and 54.43% and 293.50 kW, respectively, as indicated in the Figures 2-4 followed by the fluids R1243zf, R1336mzz(Z), R1233zd(E), R1225ye(Z), R1234ze(Z) and R1234ze(E) and R1234yf. The curve for thermal efficiency and power output has the same pattern as the curve for exergy efficiency. The explanation behind this is that thermal efficiency is directly linked to exergy efficiency [25]. Increase in solar irradiation from 0.4 kW/m^2 to 0.95 kW/m^2, the exergy efficiency, thermal efficiency and power out of the system were increased from 36.73% to 58.52%, 34.16% to 54.42% and 183kW to 293.5kW respectively by R1224ye(Z).

Figure 2. Variation of Exergy efficiency with DNI

Figure 3. Variation of thermal efficiency with DNI

Figure 4. Variation of power output with DNI

Figure 6. variation of thermal efficiency with concentration ratio
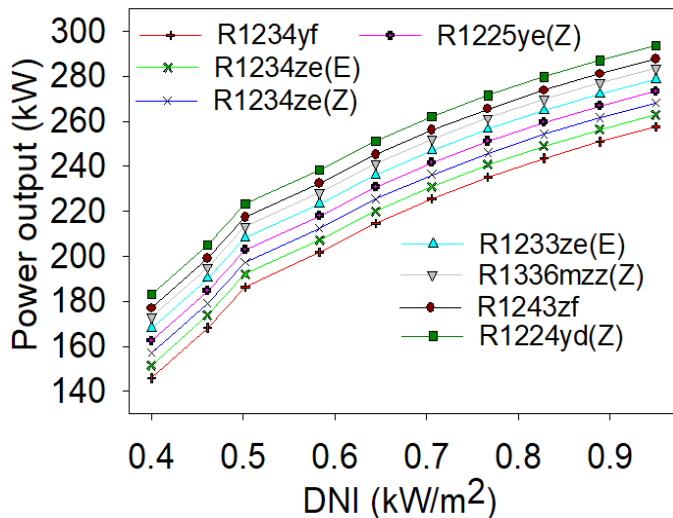
3.2 Influence of concentration ratio on the system performance

Another receiver design parameter to consider is the concentration ratio, which has an impact on the combined system's performance. As illustrated in Figures 5-7, increasing the concentration ratio increases combined cycle exergy efficiency and thermal efficiency. As the concentration ratio rises, the receiver efficiency rises, causing the HTF outlet temperature to rise, as the turbine inlet temperature is inversely proportional to the receiver outlet temperature. As a result, as the temperature of the turbine inlet grew, the combined cycle efficiency increased. The fluid R1224yd(Z) achieved the highest exergy efficiency, thermal efficiency and power output once again. Exergy efficiency, thermal efficiency and power output increased from 38.76% to 59.89%, 36.05% to 55.70% and 143.2kW to 342.7kW, respectively, based on R1224yd(Z) when the concentration ratio is increased from 200 to 1400 as shown in figures 5-7.
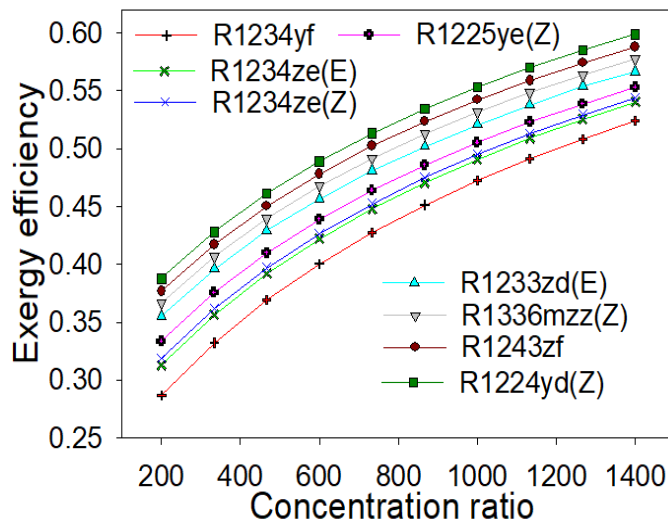

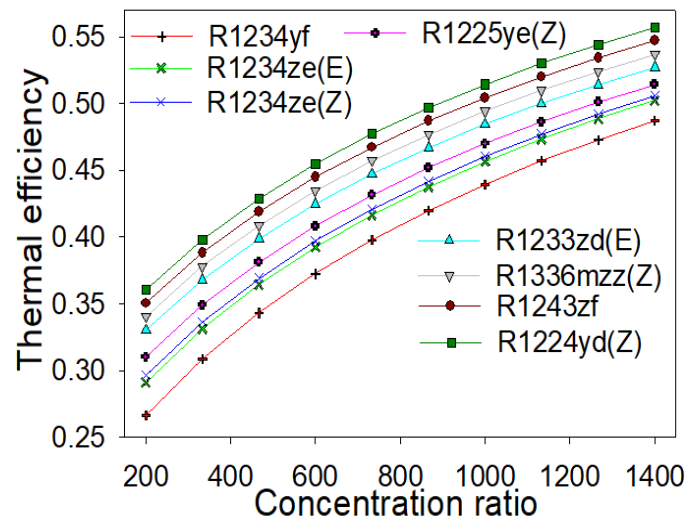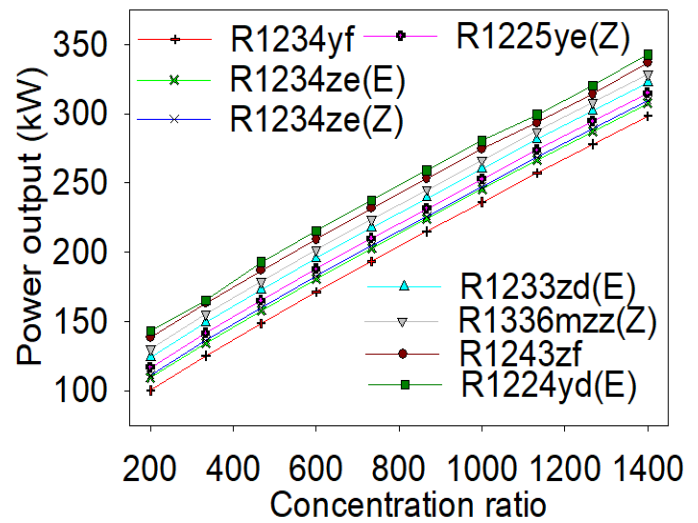*Figure 7. Variation of power output with concentration ratio*

3.3 Influence of HTF velocity on system performance

Figures 8-10 show the variation of exergy efficiency, thermal efficiency and power output with HTF velocity in absorber tube. From figure it can be seen that both efficiencies increase with velocity. Reason for increase in second law efficiency with the velocity is that due to increases in velocity of fluid Reynolds number is increased consequently convective heat transfer coefficient increased so much heat is carried with heat transfer fluids so much heat available with HTF. This leads to increase in efficiencies. Highest exergy efficiency, thermal efficiency and power output were obtained for R1224yd(Z) and varies 56.60% to 58.0%, 52.63% to 54.03% and 289.7 to 292.3 kW respectively when velocity varies from 0.01(m/s) to 0.1(m/s) and while lowest values were obtained by the R1234yf among other considered working fluids, it varies from 47.83% to 48.88%, 44.48% to 45.45% and 242.5 to 243.2kW respectively when it velocity varies from 0.01(m/s) to 0.1(m/s).

Figure 5. Variation of exergy efficiency with concentration ratio

It was seen that performance improvement slightly varied with the velocity due to effect of standalone cycle only. The performance of bottoming ORC did not affect significantly.
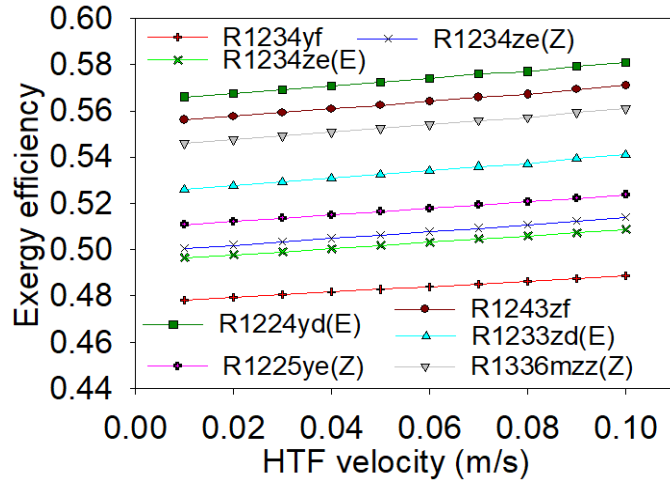
3.4 Influence of receiver emittance on system performance

Receiver emittance is the important parameter to be examined because it affects the receiver performance. It is seen in figure 11-13, performance of the combined cycle decreases with the receiver emittance. Receiver's surface temperature is the function of the receiver emittance. Receiver efficiency decreases with the receiver emittance according to Eq. (4). That means more heat loss to the surrounding, consequently less heat energy available to the combined cycle. This leads to decrease in the both efficiencies of the combined cycle. Increase in solar emittance from 0.05 to 0.2 reduces the exergy efficiency, thermal efficiency and output power of the system from 61.22% to 59.66%, 57.29% to 55.84% and 286.4kW to 278.8kW respectively based on the R1224yd(Z) as shown in Figures 11-13. Therefore, it becomes necessary to decrease the solar emittance while designing the SPT to get better performance of combined cycle for power generation.
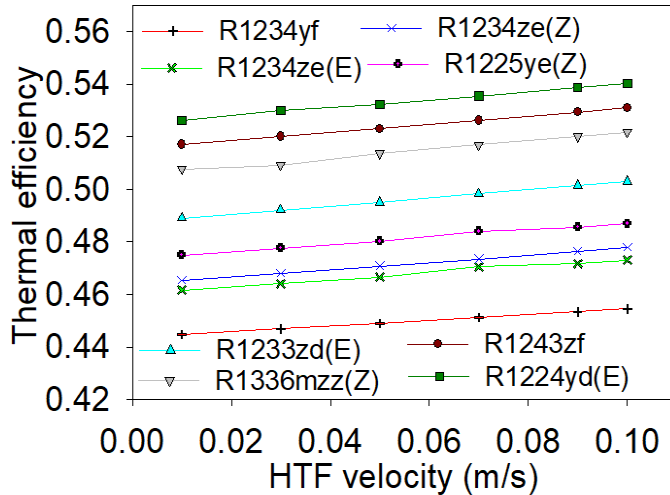

Figure 8. Variation of exergy efficiency with HTF velocity

Figure 9. Variation of thermal efficiency with HTF velocity

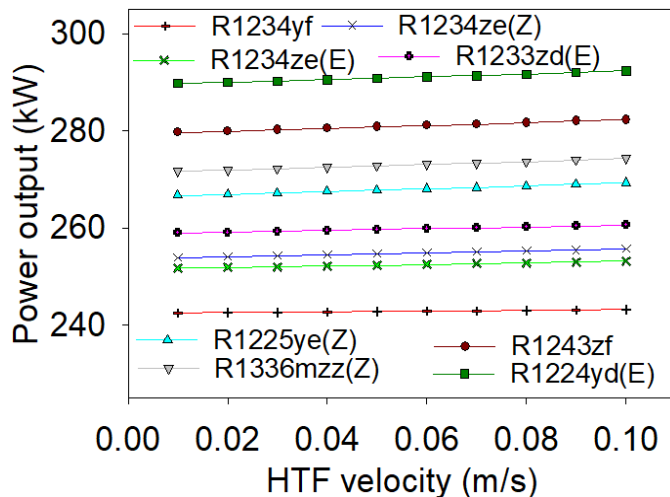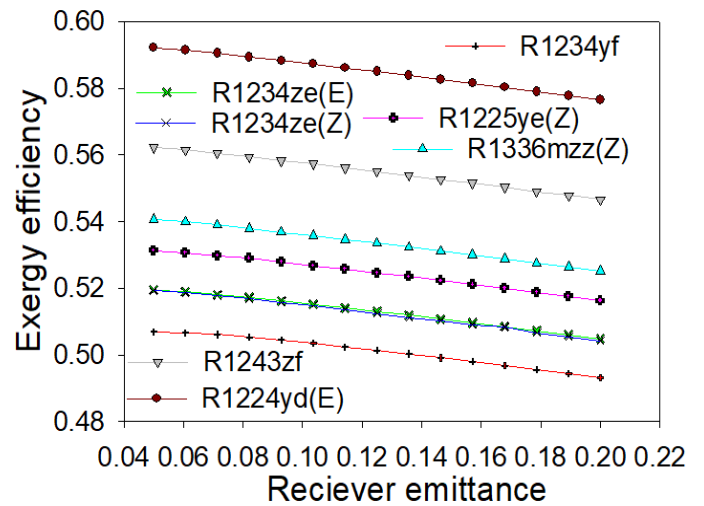*Figure 10. Variation of power output with HTF velocity*

Figure 11. Variation of exergy efficiency with receiver emittance
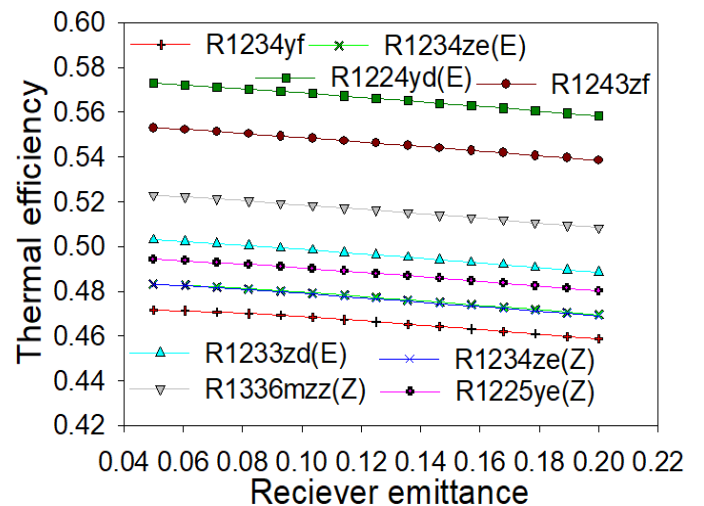

Figure 12. Variation of thermal efficiency with receiver emittance
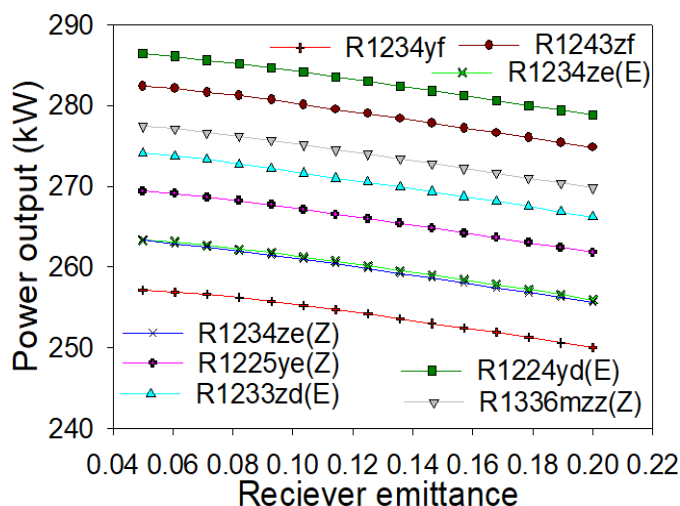
297

Figure 13. Variation of power output with receiver emittance

Conclusions

- Performance of the system increased with the DNI. Maximum performance of combined cycle was found with R1224yd(E) fluid followed by R1243zf, R1336mzz(Z), R1233zd(E), R1225ye(Z), R1234ze(Z), R1234ze(E) and R1234yf at present input conditions. Maximum exergy efficiency, thermal efficiency and output power were increased from 36.73% to 58.52%, 34.16% to 54.42% and 183kW to 293.5kW respectively when DNI increased from 0.4 kW/m^2 to 0.95 kW/m^2 based on R1224yd(Z) fluid.

- Increase in concentration ratio from 200 to 1400 increases the highest thermal and exergy efficiency and output power increased from 38.76% to 59.89%, 36.05% to 55.70% and 143.2kW to 342.7kW with fluid R1224yd(Z).

- Performance of combined cycle increased with velocity of HTF in receiver. Highest exergy efficiency, thermal efficiency and power output were obtained for R1224yd(Z) and varies 56.60% to 58.1%, 52.92% to 54.4% and 289.7 to 292.3kW respectively when velocity varies from 0.01(m/s) to 0.1(m/s).

- Apart from this R1224yd(Z) may be recommended for better performance of the combined cycle based on current input conditions.

- Current study limited to the parametric analysis and effects evaluation of few selected SPT design parameters on combined cycle. Further, this system can be analyzed with more SPT design parameters.

References

[1]   Khan Y, Mishra RS. Thermo-economic analysis of the combined solar based pre-compression supercritical CO_2 cycle and organic Rankine cycle using ultra low GWP fluids. Thermal Science and Engineering Progress 2021; 23:100925.doi.10.1016/j.tsep.2021.100925.

[2]   Khan Y, Mishra RS. Performance analysis of solar driven combined recompression main compressor intercooling supercritical CO_2 cycle and organic Rankine cycle using low GWP fluids. Energy and Built Environment 2021.doi.10.1016/j.enbenv.2021.05.004.

[3]   Farges O, Bézian J, El-Hafi M. Global optimization of solar power tower systems using a Monte Carlo algorithm: Application to a redesign of the PS10 solar thermal power plant. Renewable Energy 2018;119:345-53.

[4]   Khatoon S, Kim M. Performance analysis of carbon dioxide based combined power cycle for concentrating solar power. Energy Conversion and Management 2020.doi: 10.1016/j.enconman.2019.112416.

[5]   Khan Y, Mishra RS. Performance evaluation of solar-based combined pre-compression supercritical CO_2 cycle and organic Rankine cycle. International journal of Green energy 2020. doi:10.1080/15435075.2020.1847115.

[6]   Alsagri AS, Chiasson A, Gadalla M. Viability Assessment of a Concentrated Solar Power Tower with a Supercritical CO2 Brayton Cycle Power Plant. Journal of Solar Energy Engineering 2018. doi:10.1115/1.4043515

[7]   Ma Y, Morozyuk T, Liu M, Yan J, Liu J. Optimal integration of recompression supercritical CO_2 Brayton cycle with main compression intercooling in solar power tower system based on exergoeconomic approach. Applied Energy 2019; 242:1134-54.

[8]   Shukla AK., Sharma A, Sharma M, Nandan G.Thermodynamic investigation of solar energy-based   triple combined power cycle, Energy Sources, Part A: Recovery, Utilization, and Environmental Effects 2018. doi: 10.1080/15567036.2018.1544995.

[9]   Abid M, Adebayo VO, Atikol U. Energetic and exegetic analysis of a novel multi-generation system using solar power tower. International journal of exergy 2019.doi:10.1504/IJEX.2019.100364

[10] Ahn Y, Bae SJ, Kim M, Cho SK, Baik S, Lee JI, Cha JE. Review of supercritical CO_2 power cycle technology and current status of research and development, Nuclear Engineering Technology 2015;47: 647–61.

[11] Singh, H., and R. S. Mishra. 2018. Performance analysis of solar parabolic trough collectors driven combined supercritical CO2 and organic Rankine cycle. Engineering Science and Technology, an International Journal 21:451–44. doi:10.1016/j.jestch.2018.03.015.

[12] Singh, H. and R.S. Mishra. 2018. Energy and exergy-based performance evaluation of solar powered combined cycle (recompression supercritical carbon dioxide cycle/organic Rankine cycle). Clean Energy, 2018, 1–14.

[13] Mishra, R.S and H. Singh. 2018. Detailed parametric analysis of solar driven supercritical CO_2 based combined cycle for power generation, cooling and heating effect by vapor absorption refrigeration as a bottoming cycle. Thermal Science and Engineering Progress 8:397–410.

[14] Khan Y, Mishra RS. Parametric (exergy-energy) analysis of parabolic trough solar collector-driven combined partial heating supercritical CO_2 cycle and organic Rankine cycle. Energy sources, part a: recovery, utilization, and environmental effects 2020.doi:10.1080/155

[15] HüseyinYağlı, YıldızKoç, and Hüseyin Kalay. 2021. Optimisation and exergy analysis of an organic Rankine cycle (ORC) used as a bottoming cycle in a cogeneration system producing steam and power Sustainable Energy Technologies and Assessments. 44:100985.

[16] Jian Song , Xiaoya Li , Kai Wang , Christos N. Markides. 2020. Parametric optimization of a combined supercritical CO2 (S-CO2) cycle and organic Rankine cycle (ORC) system for internal combustion engine (ICE) waste-heat recovery. Energy Conversion and Management, 218:112999.

[17] Reyes-Belmonte, M.A., A. Sebastián, and M. Romero.2016.Optimization of a recompression supercritical carbon dioxide cycle for an innovative central receiver solar power plant. Energy.112 :17–27.

[18] Polimeni, S., M. Binotti, L. Moretti, and G. Manzolini. 2018. Comparison of sodium and KCl-MgC$_{12}$ as heat transfer fluids in CSP solar tower with SCO$_2$ power cycles. Solar Energy.162:51024.

[19] Bejan A, Kearney DW, Kreith F. Second law analysis and synthesis of solar collector systems. J. Sol. Energy Eng. Trans. ASME 1981;103:23–28.

[20] Ho CK., Iverson BD. Review of high-temperature central receiver designs for concentrating solar power. Renewable Sustainable Energy Reviews 2014;29:835–46.

[21] Wang X, Liu Q, Lei J, Han W, Jin H. Investigation of thermodynamic performances for two-stage recompression supercritical CO2 Brayton

cycle with high temperature thermal energy storage system. Energy Conversion Management 2018;165:477–87.

[22] Neises T, Turchi C. A Comparison of Supercritical Carbon Dioxide Power Cycle Configurations with an Emphasis on CSP Applications. Energy Procedia 2014;49:1187–96.

[23] Song J, Li X, Ren X, Gu C. Performance analysis and parametric optimization of supercritical carbon dioxide (S-CO2) cycle with bottoming Organic Rankine Cycle (ORC). Energy 2018;143:406-16.

[24] Cengel YA, Boles MA. Thermodynamics An Engineering Approach. 5th edition;McGraw-Hill publication. New York;2004.

[25] R. Petela, Exergy analysis of the solar cylindrical-parabolic cooker, Sol. Energy 79 (2005) 221–233.

[26] Klein SA. Engineering Equation Solver (EES), Academic Commercial V7.714. F-Chart Software 2020, www.fChart.com.

[27] Koc,Y., H. Yagli, and A. Koc. 2019. Exergy analysis and performance improvement of a subcritical/supercritical Organic Rankine Cycle (ORC) for exhaust gas waste heat recovery in a biogas fuelled Combined Heat and Power (CHP) 520 engine through the use of regeneration. Energies 12 (4):575. doi:10.3390/en12040575.

[28] Moloney, F., E. Almatrafi, D.Y. Goswami. 2017.Working fluids parametric analysis for the regenerative supercritical organic Rankine cycle for medium geothermal reservoir temperatures. Energy Procedia.129:599- 606.

[29] Calm,J.M.(1994):Referegerant safety. ASHRAE Journal.36.(7):17-26.

[30] Al-Sulaiman FA. Exergy analysis of parabolic trough solar collectors integrated with combined steam and organic Rankine cycles. Energy Conversion and Management 2014;77:441–49.

[31] Khan Y and Mishra RS. 2021. Performance comparison of basic and parallel double evaporator organic rankine cycle integrated with solar based supercritical CO_2 cycle. Journal of Thermal Engineering. (accepted)

Nomenclature

$\dot{E}_{solar}$	Solar exergy (kW)
$\dot{Q}_h$	Actual solar heat received by heliostat field (kW)
$\dot{Q}_{loss,r}$	Heat loss from the receiver (kW)
$\dot{Q}_r$	Heat received by central receiver (kW)
$\dot{Q}_{solar}$	Solar heat received by heliostat field (kW)
A_h	Heliostat area (m^2)
$\dot{E}$	Exergy rate (kW)
$\dot{E}D$	Rate of exergy destruction (kW)
f_{view}	Receiver's view factor
h_{conv}	Coefficient for convection heat loss (W/ m^2-K)
$\dot{m}$	Mass flow rate (kg/s)
N_h	Number of heliostat
$\dot{Q}$	Heat rate in (kW)
T_R	Receiver surface temperature (K)
$\dot{W}$	Power (kW)

η_{ex}	Exergy efficiency
η_h	Heliostat efficiency
η_r	Receiver thermal efficiency
η_{th}	Thermal efficiency
Cp	Specific heat (kJ/kg-K)
DNI	Direct normal irradiation (W/m^2)
h	specific enthalpy (kJ/kg)
s	specific entropy (kJ/kg-K)
SCO_2	Supercritical carbon dioxide
T	Temperature (K)

Abbreviations

Comp	Compressor
Cond	condenser
CR	concentration ratio
CV	Control volume
HEX1	heat exchanger-1
HEX2	heat exchanger-2
ORC	Organic Rankine cycle
OT	ORC turbine
recup	Low temperature recuperator
SPT	solar power tower

Subscripts

e	exit
0	dead condition
r	receiver
h	heliostat
i	inlet
j	particular state
su	Sun
ms	molten salt

Greek letters

η	Efficiency
ε	Effectiveness
α	Solar absorbance
δ	Change in property
β	Sun's subtended cone half angle(rad)
σ	Stephen Boltzmann constant (W/m)